JOURNAL OF CATALYSIS **176,** 42–51 (1998)
ARTICLE NO. CA982001

Catalytic Properties of γ-Alumina-Supported Pt Catalysts for Tetralin Hydrogenation

Effects of Sulfur-Poisoning and Hydrogen Reactivation

J.-R. Chang[1] and S.-L. Chang

Department of Chemical Engineering, National Chung Cheng University, Chia-Yi, Taiwan, Republic of China

Received March 14, 1997; revised December 1, 1997; accepted January 5, 1998

Tetralin hydrogenation was chosen as a model reaction for aromatics reduction reaction. The effects of sulfur-poisoning on the catalytic properties of γ-alumina-supported Pt catalysts were investigated by kinetic studies carried out in a continuous fixed-bed reactor at 543 K, under 32 atm total pressure, and weight hourly space velocity (WHSV) ranging from 2.0 to 12 h^{-1}. An empirical power-law rate reaction was used to model the reaction kinetics. Parameter estimation results indicated that both the reaction order and rate constant decreased with increasing sulfur concentration; 500 ppm sulfur-poisoned catalysts were reactivated by hydrogen treatment at 723 and 823 K, respectively. The electronic properties of fresh, sulfur-poisoned, and hydrogen-reactivated catalysts were investigated by fast Fourier transform infrared (FT-IR) spectroscopy characterizing CO adsorbed on the catalysts. The results indicated that the bond strength between CO and platinum was weakened with the increase of sulfur-poisoning, suggesting that the adsorption of H_2S and/or the formation of PtS decreased electronic density of Pt clusters. The electronic density can be regained by hydrogen reactivation, indicated by the results of FT-IR and X-ray absorption near-edge structures (XANES) spectroscopy. The decrease of reaction order with the severity of sulfur-poisoning may have resulted from the decrease of electronic density of the Pt clusters and thus can be recovered with hydrogen reactivation. In contrast, the activity of the sulfur-poisoned catalyst was not fully recovered because of the sulfur-poisoning induced Pt agglomeration and the residue sulfur deposited on Pt sites, inferred from the EXAFS, FT-IR, and chemical analysis results. The comparison of the structure between the sulfur-poisoned and the hydrogen-reactivated catalysts indicates that the adsorbed H_2S was removed at 723 K, while the morphology of the Pt clusters had no significant changes after the hydrogen treatment; hydrogen reactivation is unable to redisperse the catalysts.

INTRODUCTION

Aromatics in diesel fuel not only lower the fuel quality, but produce undesired emissions in exhaust gases. The growing understanding of the health hazard associated with these emissions is leading to limitation on aromatics in both Europe and the United States (1, 2). Even though there are a number of differences among the specifications of individual countries, it has been a general trend to reduce aromatics in diesel. However, studies have shown that existing hydrotreating processes can only reduce the aromatics to the margin of specification (3). In order to meet the gradually stricter diesel fuel standard, refiners have to develop new catalyst systems and hydrotreating processes.

The hydrogenation of aromatics is a reversible reaction in which polynuclear aromatics are first converted to dinuclear aromatics, then to mononuclear aromatics, which are in turn converted to naphthenes. Among the reaction steps, hydrogenation of the monoaromatics is the most difficult one (4). With supported Pt catalysts, the reaction can be carried out at relatively low temperature, compared with conventional hydrotreating catalysts; lower temperature is also thermodynamically favorable for aromatics saturation. However, because of low sulfur resistance of the Pt catalysts, prior to the reaction, a severe hydrotreating is necessary to reduce the feedstock sulfur below certain minimum limits (few ppm for γ-alumina supported Pt catalysts) (5). From an industrial perspective, the severe hydrotreating is economically unfavorable. Thus, increasing thiotolerance and developing a regeneration scheme are very crucial in improving the Pt catalysts for industrial application.

The goal of this research was to investigate the relation between sulfur-poisoning and catalytic properties of Pt/γ-Al_2O_3 catalysts. In addition, sulfur-poisoned catalysts were reactivated by hydrogen treatment at 723 and 823 K, to investigate the possibility of hydrogen reactivation being used for the regeneration of sulfur-poisoned catalysts. Tetralin hydrogenation was chosen as a model reaction and benzothiophene was chosen as the model compound for sulfur poisoning. The reasons for the choice of these two compounds were reported in the previous paper (6). Kinetics of tetralin hydrogenation were correlated with the electronic

[1] Correspondence to J.-R. Chang.

0021-9517/98 $25.00

properties and structure of the fresh, the sulfur-poisoned, and the hydrogen-reactivated catalysts. The structures of the sulfur-poisoned and the hydrogen-reactivated catalysts were characterized by extended X-ray absorption fine structure (EXAFS) spectroscopy and CO chemisorption. Electron properties of the catalysts were examined by X-ray absorption near edge structure (XANES) spectroscopy and by fast Fourier transform infrared (FT-IR) spectroscopy characterizing CO adsorbed on the catalysts.

EXPERIMENTAL

Materials and catalyst preparation. The catalyst samples were prepared by impregnation technique. The γ-Al_2O_3 samples (A2U, γ-Al_2O_3, with surface area about 170 m^2/g, purchased from Osaka Yogyo) were brought in contact with a solution of [H_2PtCl_6] (Strem, 99.9%) in doubly distilled deionized water, followed with evacuation at room temperature under vacuum, and then calcined at 723 K for 4 h. The catalyst sample contained 0.92 ± 0.02 wt% Pt, as measured by inductively coupled plasma optical emission spectroscopy with a Jarnell–Ash 1100 instrument.

Catalytic performance. The catalytic performance tests were carried out with a continuous downflow fixed-bed reaction system. The reactor was a stainless steel tube with an inside diameter of 1.2 cm. It was heated electrically and the temperature controlled by a PID temperature controller with a sensor at the outer wall of the reactor. The temperature difference between the outer reactor wall and the center of the catalyst bed was about 15°C. The upstream part of the reactor was filled with particles of inactive ceramic material for preheating the H_2 and hydrocarbon mixture. The reaction system was first purged with dry nitrogen gas for 2 h. Catalyst samples with pellet diameter about 1.2 mm of 1.5 g were diluted with inert ceramic in a ratio of 1 : 5 (particle size about 200 μm) then reduced at 723 K under 32 atm pure hydrogen for 4 h. Before the reaction, tetralin (Merck, >98%) was dried with particles of activated 4 Å molecular sieve. To investigate the effects of sulfur poisoning on the catalytic performance, dry tetralin was mixed with benzothiophene to prepare feed of 0 to 1000 ppm sulfur content. Sulfur-poisoning of the catalysts was then carried out with a weight hourly space velocity (WHSV) 4.8 (g of feed/h · g of catalyst) with hydrogen flow rate of 100 mL/min., at 543 K under 32 atm total pressure. When tetralin conversion showed no significant changes (about 24 h), kinetic studies were conducted, with WHSV ranging from 2.0 to 12 h^{-1}. Liquid products were trapped by a condenser at 268 K. Samples were collected periodically and analyzed by gas chromatography. A Shimadzu model GC-14B gas chromatography equipped with a 10% OV-101 on Chrom W-HP 80/100 mesh column of 18 m × 0.22 mm ID and FID detector was used for feed and reacted sample analysis. The column was operated at 383 K with linear velocity 20 cm/min dry nitrogen. The material balance is about 98% (±3%) for the catalytic performance tests.

The Pt catalyst treated with 500 ppm sulfur for 24 h, was used as a sulfur-poisoned catalyst sample to study the hydrogen reactivation effects. The reactivation process was performed with hydrogen flow rate of 100 mL/min under 32 atm total pressure and at temperature of 723 or 823 K for 2 h. The activity of the reactivated catalysts was examined by the kinetic study of tetralin hydrogenation.

After each experiment, the system was wetted with hexane at room temperature for 2 h, unloaded in air, and then stored in nitrogen-filled sealed vials using a double manifold Schlenk vacuum line. Before the storage, the catalyst samples were exposed to air for about 0.5 h. The hexane treatment is to protect the platinum clusters from oxidation by providing resistance to mass transfer of oxygen; it minimize the surface contamination during catalyst unloading. As observed in the past, without hexane treatment, a EXAFS peak at 2.05 Å has been detected for the used catalyst samples. Since this peak is consistent with the Pt–O bond distance of α-PtO_2, it indicates the oxidation of the catalysts.

By wetting the catalysts with hexane, no such Pt–O contribution has been detected. Thus, the air contamination of the catalyst sample was regarded as eliminated.

In order to remove sulfur contamination from reaction apparatus, the reactor was treated by heating at 873 K for 8 h in flowing air. Since the reactor is made of stainless steel 316, sulfur, or more precisely, hydrogen sulfide formed during the reaction causes the formation of iron sulfide according to the balanced reaction:

$$H_2S + Fe \Leftrightarrow FeS + H_2.$$

When the apparatus was treated at 873 K in flowing air, the ferrous sulfide was oxidized into ferric sulfate and then decomposed into ferric oxide Fe_2O_3 and sulfur oxides (SO_2 and SO_3). The sulphur oxides thus formed then were removed by NaOH scrubbing and the red ferric oxide were removed by brushing.

By this treatment, the sulfur contamination of the apparatus is evidently removed. As shown in the previous paper (6), the blank test and EXAFS characterizing the initial fresh catalyst sample indicated that no catalyst deactivation being observed during blank test and no Pt–S contributions being detected for the initial fresh catalyst sample.

Catalyst Characterization

CO chemisorption. A stainless tube was packed with 1 g of catalyst sample. The fresh catalyst sample was reduced at the same operating conditions as those for catalytic performance test, the sulfur-poisoned catalyst samples were pretreated with a He purge at 393 K, and the hydrogen-reactivated catalysts were pretreated under the same operating conditions used in hydrogen reactivation. After the

treatments, the tube was then attached to a Shimadzu model GC-14B gas chromatography with a thermal conductivity detector (TCD). The tube for adsorption measurement was connected with a three-way ball valve and the connection ports were carefully purged with He gas before adsorption experiments to inhibit any air contamination. After the system became steady (20 mL/min He flow rate and 308 K), 0.1 mL pulse of CO was repeatedly injected into catalyst bed with He carrier gas until none of the pulse was chemisorbed. The amount of chemisorption was then calculated by summing up the proportions of all pulses consumed.

Characterization of catalyst samples by FT-IR. Infrared Fourier transform spectroscopy characterizing CO adsorbed and sulfur deposited on the catalysts was recorded with a Shimadzu SSU-8000 instrument having a spectral resolution of 4 cm^{-1}. The wafer samples were loaded into a IR cell. The cell was designed allowing us to connect to a vacuum/gas-handling manifold for *in-situ* treatment. The fresh and hydrogen-reactivated catalyst samples were pretreated at the same temperature and hydrogen flow rate as those for catalytic performance test but at 1 atm. After the treatments, the samples were cooled from the treatment temperature ($\geq$723 K) to room temperature with He flowing at 20 mL/min, and CO (flowing at 50–100 mL/min at 1 atm) was introduced into the cell and maintained for about 20 min. After the CO treatment, the cell was evacuated to a pressure of approximately 10^{-3} Torr, and IR spectra were recorded. For the sulfur-poisoned catalysts, the samples were treated with flowing He (20 mL/min) to purge the hexane soaked in the catalysts. After introducing CO to the IR cell and following with evacuation, IR spectra were recorded.

FT-IR was also used to characterize the sulfur coverage of the 500 ppm sulfur-poisoned and of the 823 K hydrogen-reactivated catalyst samples. The samples were loaded into a IR cell and then purged in N_2 flowing at about 50 mL(NTP)/min for 30 min. The transformation of sulfur on the catalysts into sulfate species linked to the alumina support was carried out by treating the samples with pure oxygen in a static condition (1 atm) at 623 K for 3 h (18). After evacuation at the same temperature for 1 h, the samples were cooled to room temperature and the IR spectra were recorded.

X-ray absorption spectroscopy. The X-ray absorption measurements were performed on X-ray beamline X-11A of the National Synchrotron Light Source (NSLS) at Brookhaven National Laboratory with a storage ring energy of 2.5 GeV and a beam current between 150 and 250 mA. A Si(111) double-crystal monochromator was used for energy selection, and it was detuned 20% at 11,614 eV to suppress higher harmonic radiation; resolution $\Delta E/E$, was estimated to be 2.0×10^{-4}. The monochromator was scanned in energy from 200 eV below the platinum L_{III} absorption edge (11564 eV) to 1200 eV above the edge. A sulfur-poisoned catalyst sample, treated with 1000 ppm sulfur for 24 h, was reactivated by hydrogen at 723 K for 2 h and then pressed into a self-supporting wafer in a N_2-filled glovebag, with the wafer thickness chosen to give an absorbance of 2.5 and measured in a transmission mode at liquid nitrogen temperature. The transmission measurement geometry was arranged using gas-filled ionization chambers to monitor the intensities of the incident and transmitted X rays. In order to gain the proper absorption ratio for the incoming X rays, the gas compositions in the ionization chamber were selected as argon 3 mL/min with nitrogen 60 mL/min at the first chamber and as argon 18 mL/min with nitrogen 24 mL/min for the second chamber, respectively.

RESULTS

Mass transfer limitation. In order to examine internal diffusion limitation, a test was performed with four different sizes of the γ-Al_2O_3 supported Pt catalyst. The results are shown in Fig. 1, where the curves for the catalyst with pellet diameter less than 2 mm are coincident (within 5% deviation), whereas the turnover frequency for the catalyst with pellet diameter of 4 mm is lower than that by the other catalyst samples.

The external mass transfer limitation was examined by the tetralin hydrogenation over the supported Pt catalyst with pellet diameter of 1.2 mm, carried out at constant WHSV (4.8 h^{-1}) with superficial mass velocity ranging from 2 to 10 mg/cm^2 s. Figure 2 shows that the conversion of tetralin was increased with superficial mass velocity.

Catalytic performance. In the previous paper (6), the total conversion of tetralin is shown as a function of time on-stream in the flow reactor for the feed containing 1000

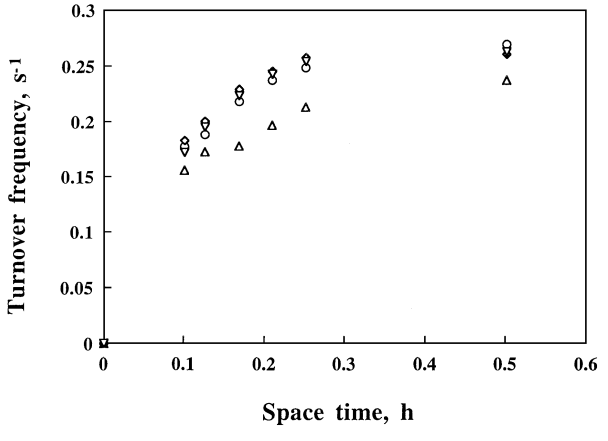

FIG. 1. Test for internal diffusion resistance by examining the turnover frequency at 543 K, H_2/Oil mol ratio of 4.5, WHSV ranging from 2.0 to 10.0, and 480 psig for tetralin conversion catalyzed by the fresh Pt/γ-Al_2O_3 catalysts of different diameter: ▽, 0.5 mm; ○, 1.2 mm; ◇, 2 mm; △, 4 mm.

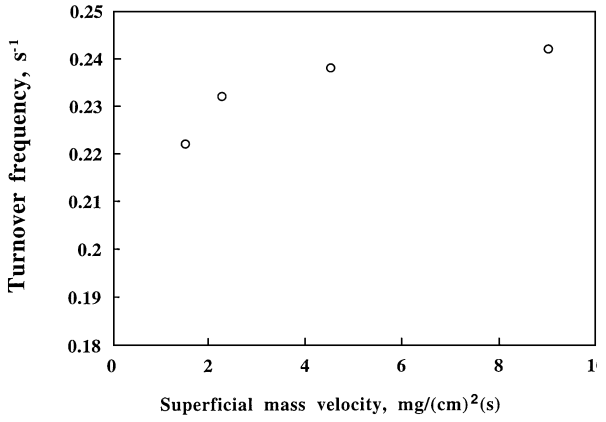

FIG. 2. Test for the external diffusion resistance by examining the turnover frequency with varying superficial mass velocity at 543 K, WHSV = 4.8 h^{-1}, and 480 psig for tetralin conversion catalyzed by the fresh Pt/γ-Al_2O_3 catalysts with diameter of 1.2 mm; the superficial mass velocity was varied by changing feed rate and amount of catalysts concomitantly so as to keep WHSV constant and the calculation of the velocity was based on the reactor inside diameter of 1.2 cm with void fraction of catalyst bed of 0.38.

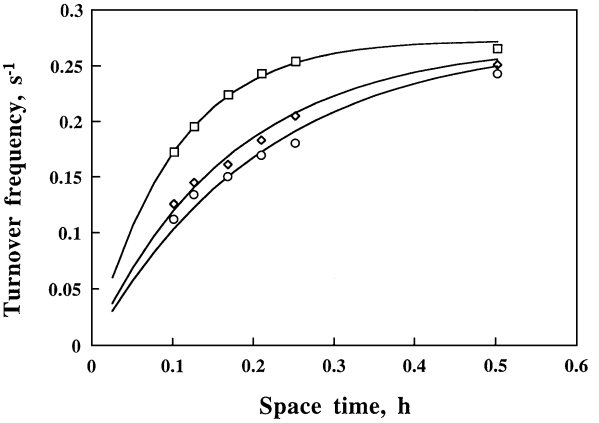

FIG. 4. Turnover frequency at 543 K and 480 psig catalyzed by the fresh and the 500 ppm sulfur-poisoned Pt/γ-Al_2O_3 catalysts after hydrogen reactivation: □, fresh catalyst; ◇, reactivation temperature = 823 K; ○, reactivation temperature = 723 K; solid lines are the data calculated from model and the calculation of the turnover frequency was based on initial Pt surface atoms.

and 2000 ppm sulfur. After catalyst deactivation became insignificant (about 24 h), kinetic studies of tetralin hydrogenation were conducted at various WHSV. As shown in Fig. 3, the turnover frequency increased with space time (1/WHSV) but decreased with the severity of sulfur poisoning.

The comparison of turnover frequency for the hydrogen-reactivated and fresh catalysts is shown in Fig. 4. The results indicated that the catalyst activity of the sulfur-poisoned catalysts was only partially recovered and it increased with increasing reactivation temperature.

Infrared spectra. The FT-IR spectra characterizing the transformation of sulfur on the catalysts into sulfate species are shown in Fig. 5. For the 500 ppm sulfur-poisoned catalyst sample, a characteristic peak of sulfate species at 1388 cm^{-1} was observed. After hydrogen reactivation at 823 K, the intensity of the peak decreased to about 20% of its original values.

As shown in Fig. 6, FT-IR peak characterizing CO adsorbed on Pt clusters of the fresh catalyst sample appeared only one peak at 2060 cm^{-1}. In contrast, an additional peak was observed for the sulfur-poisoned catalyst samples and the absorption frequency of this peak increases with the severity of sulfur poisoning (2065 cm^{-1} for 100 ppm

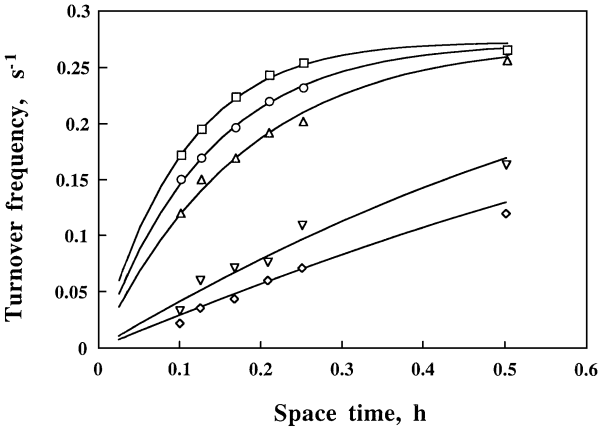

FIG. 3. Turnover frequency at 543 K and 480 psig catalyzed by the fresh and sulfur-poisoned Pt/γ-Al_2O_3 catalysts: □, fresh catalyst; ○, sulfur = 100 ppm; △, sulfur = 250 ppm; ▽, sulfur = 500 ppm; ◇, sulfur = 1000 ppm; solid lines are the data calculated from model and the calculation of the turnover frequency was based on initial Pt surface atoms.

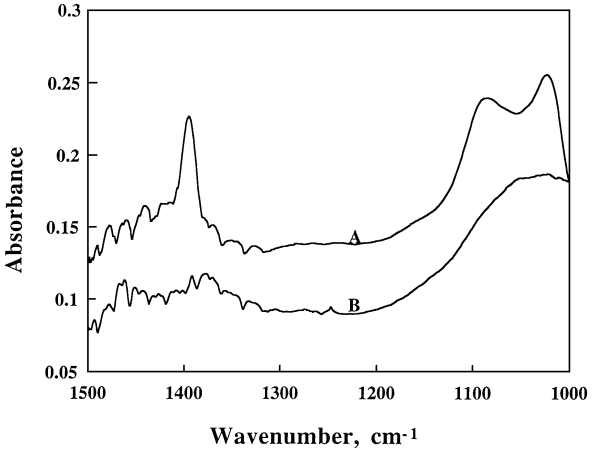

FIG. 5. Infrared spectra characterizing the sulfate species formed by treating the catalysts with pure oxygen at 623 K: (a) the 500 ppm sulfur-poisoned Pt/γ-Al_2O_3 catalysts and (b) the catalyst after 823 K hydrogenation reactivation.

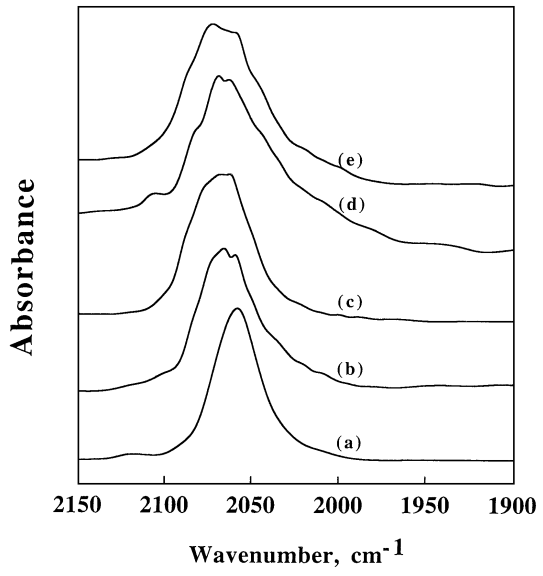

FIG. 6. Infrared spectra in the ν_{CO} stretching region characterizing the CO adsorbed on the fresh and the sulfur-poisoned Pt/γ-Al_2O_3 catalysts: (a) fresh catalyst; (b) sulfur = 100 ppm; (c) sulfur = 250 ppm; (d) sulfur = 500 ppm; (e) sulfur = 1000 ppm.

sulfur-poisoned catalyst sample and 2075 cm^{-1} for 1000 ppm sulfur-poisoned catalyst sample).

The infrared absorption bands of the CO adsorbed on the 500 ppm sulfur-poisoned catalyst sample were peaked at 2060 and 2070 cm^{-1}. The band intensity of the peak at 2070 cm^{-1} decreased with the increase of hydrogen reactivation temperature (Fig. 7).

X-ray absorption near edge structure (XANES) spectra. The normalized Pt L_{III} absorption edge data characterizing of the sulfur-poisoned (1000 ppm sulfur, 24 h) and hydrogen-reactivated catalyst samples are shown in Fig. 8. As indicated in the figure, there is a small difference between the results for two samples; the intensity of the absorption of the sulfur-poisoned catalyst sample is slightly higher than that of the hydrogen reactivated one.

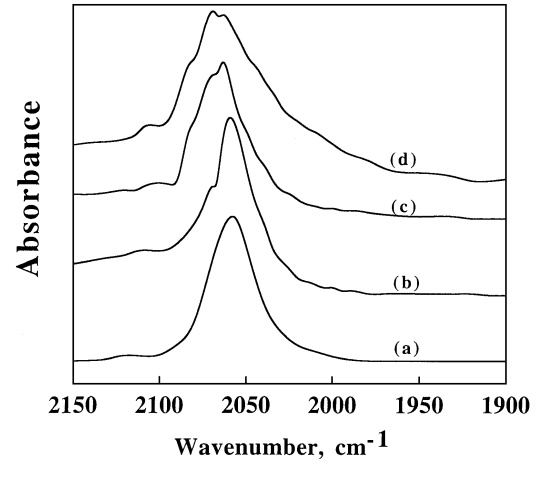

FIG. 7. Infrared spectra in the ν_{CO} stretching region characterizing the CO adsorbed on the fresh, the sulfur-poisoned, and the 500 ppm sulfur-poisoned Pt/γ-Al_2O_3 catalysts after hydrogen reactivation: (a) fresh catalyst; (b) reactivation temperature = 823 K; (c) reactivation temperature = 723 K; (d) 500 ppm sulfur-poisoned catalysts.

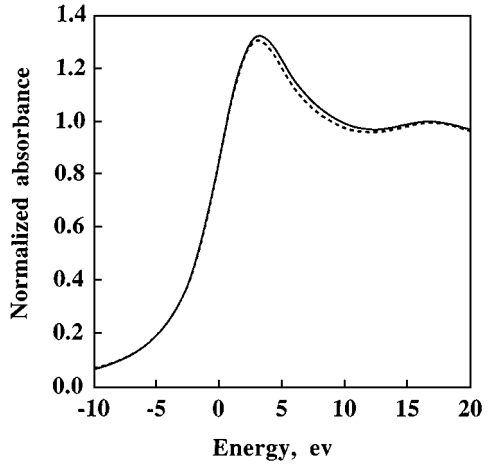

FIG. 8. Structure of the Pt L_{III} absorption edge characterizing the 1000 ppm sulfur-poisoned Pt/γ-Al_2O_3 catalysts (solid line) and the catalyst after 723 K hydrogenation reactivation (dashed line).

EXAFS spectra. The normalized EXAFS function of the hydrogen reactivated catalyst sample was obtained by a cubic spline background subtraction and normalized by the edge height (7). The raw EXAFS data have a signal-to-noise ratio >60 and the comparison of the spectra with the EXAFS spectroscopy corresponding to the initial fresh catalyst, the sulfur-poisoned catalyst, and the 723 K hydrogen-reactivated catalyst sample is shown in Fig. 9. The EXAFS data were analyzed by the difference file technique

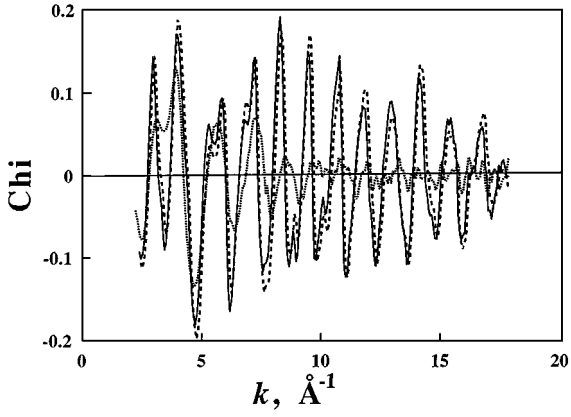

FIG. 9. k^1-weighted raw EXAFS data for the fresh catalyst (dotted line), the 1000 ppm sulfur-poisoned catalyst (dashed line), and the 1000 ppm sulfur-poisoned catalyst after 723 K hydrogenation reactivation (solid line).

TABLE 1a

EXAFS Results for the 1000 ppm Sulfur-Poisoned γ-Alumina-Supported Pt Catalyst after 723 K Hydrogen Reactivation[a]

Shell	N	R	$\Delta\sigma^2 \times 1000$	ΔE_0 (eV)	EXAFS reference
Pt–Pt	8.0 ± 0.2	2.774 ± 0.001	0.3 ± 0.2	-3.5 ± 0.1	Pt–Pt
Pt–S	2.2 ± 0.3	2.33 ± 0.01	13 ± 2	0.71	Pt–Cl
Pt–S	0.03 ± 0.04	2.53 ± 0.02	-4 ± 4	-5.1	Pt–Cl

[a] Z is the atomic number; N is the coordination number for the absorber–backscatterer pair; R is the average absorber–backscatterer distance; $\Delta\sigma^2$ is the Debye–Waller factor, and ΔE_0 is the inner potential correction. To consider the difference of absorber–backscatterer distance between the reference shell and the Pt–S shell to be analyzed, the coordination number N of the Pt–S shell is corrected by the equation, $N = N_{\text{unc}} e^{2(R_j - R_{\text{ref}})/\lambda(k)}$, where N_{unc} is determined in the EXAFS data analysis by using R_{ref} as a reference coordination distance. The number of parameters used to fit the data in this first shell is 12; the statistically justified number is approximately 13, estimated from the Nyquist theorem, $n = (2\Delta k \Delta r/\pi) + 1$, where Δk and Δr, respectively, are the k and r ranges used in the forward and inverse Fourier transform.

and nonlinear least-square multiple-shell fitting routine of Koningsberger *et al.* (7–9), and the structural parameters are summarized in Table 1a. The comparison of the data with the fit, both in k space and r space is shown in Fig. 10. The number of parameters used to fit the data in the first shell is 12; the statically justified number is approximately 13, estimated from the Nyquist theorem (10).

Coordination number, N, and relative Debye Waller factor, $\Delta\sigma^2$, are interrelated, at least in a Fourier transform. There are an infinite number of combinations, of N and $\Delta\sigma^2$ that give the same peak height in the Fourier transform. However, coordination number and Debye Waller factor both have a different k-dependence; an increasing coordination number results in an increase of amplitude of the whole k-range of EXAFS, whereas a lower Debye Waller factor will result in an increase in amplitude at higher k-value. Hence, to decouple the effects of N and $\Delta\sigma^2$, different weighted Fourier transforms have to be used; multiplication of the EXAFS function with k^1 or k^3 before the Fourier transform emphasizes the low and high k ends, respectively. In Fig. 10, both k^1 and k^3 Fourier transforms of the experimental and calculated EXAFS were presented to demonstrate that we have decoupled the interrelation between N and $\Delta\sigma^2$.

TABLE 1b

EXAFS Results for the 1000 ppm Sulfur-Poisoned γ-Alumina-Supported Pt Catalyst[a]

Shell	N	R	$\Delta\sigma^2 \times 1000$	ΔE_0 (eV)	EXAFS reference
Pt–Pt	7.3 ± 0.2	2.779 ± 0.001	0.1 ± 0.2	-4.0 ± 0.2	Pt–Pt
Pt–S	1.9 ± 0.5	2.34 ± 0.03	8 ± 5	-4.1	Pt–Cl
Pt–S	0.5 ± 0.4	2.53 ± 0.02	-4 ± 4	-5.1	Pt–Cl

[a] All footnotes are the same as in Table 1a.

DISCUSSION

Mass transfer limitations. As shown in the report of Chiou *et al.* (11), the tetralin conversion has no significant difference for the 1.2-mm diameter Pt/γ-Al_2O_3 catalysts with different average pore diameter (389 and 141 Å), concluding that the internal mass transfer limitation of the catalyst for the performance test is negligible. Examination of the internal diffusion limitation with the Pt catalyst of four different diameters is consistent with the conclusion. As shown in Fig. 1, the observed reaction rates for the catalyst with pellet diameter less than 2 mm have no significant difference, indicating that the pore diffusion limitation is negligible in the catalytic performance tests; catalysts used for the tests is of 1.2-mm diameter.

As shown in Fig. 2, the observed reaction rates were increased with superficial mass velocity for the tetralin hydrogenation over the supported Pt catalyst with the same pellet diameter and weight-hourly space velocity. The results indicated that the external mass transfer limitation cannot be neglected in the given reaction system.

Rate expression for tetralin hydrogenation over the fresh, sulfur-poisoned, and hydrogen-reactivated catalysts. According to Boudart (12), tetralin hydrogenation is a simple first-order, irreversible surface reaction. If mass transfer limitation is negligible, the rate expression can be formulated as: $k_r C_{H_2} C_T/(1 + K_T C_T)$, where C_T is the concentration of tetralin, C_{H_2} is the hydrogenation concentration in liquid phase, K_T is the tetralin adsorption equilibrium constant, and k_r is the product of K_T, K_{H_2} (hydrogen adsorption equilibrium constant), k_{sr} (surface reaction rate constant), and S^0 (total active sites): $K_r = K_T K_{H_2} k_{sr} S^0$. However, because of the difficulty in determining K_T, K_{H_2}, C_{H_2}, and the effects of external mass transfer on the reaction, instead of rigorous kinetic analysis, an empirical power-law rate equation was used to fit the kinetic data.

By using least square criteria and gradient method (13), the reaction rate constant k and the reaction order n were estimated to be 10.7 and 0.97, respectively, for the fresh catalyst sample (Table 2). Performance tests of the sulfur-poisoned catalysts indicated that the reaction rate constant was inversely proportional to sulfur concentration and the reaction order dropped from about 1.0 for the catalyst without sulfur-poisoning to about 0.5 for the catalysts with severe sulfur poisoning (sulfur in feed $\geq$500 ppm). The decrease in the rate constant is thought to be caused by the loss of active sites. The decrease in the reaction order is considered to be a consequence of the increase of tetralin-adsorption-equilibrium constant, K_T, resulting from increasing affinity between aromatics and the catalysts. A zero-order reaction for the reduction of aromatics

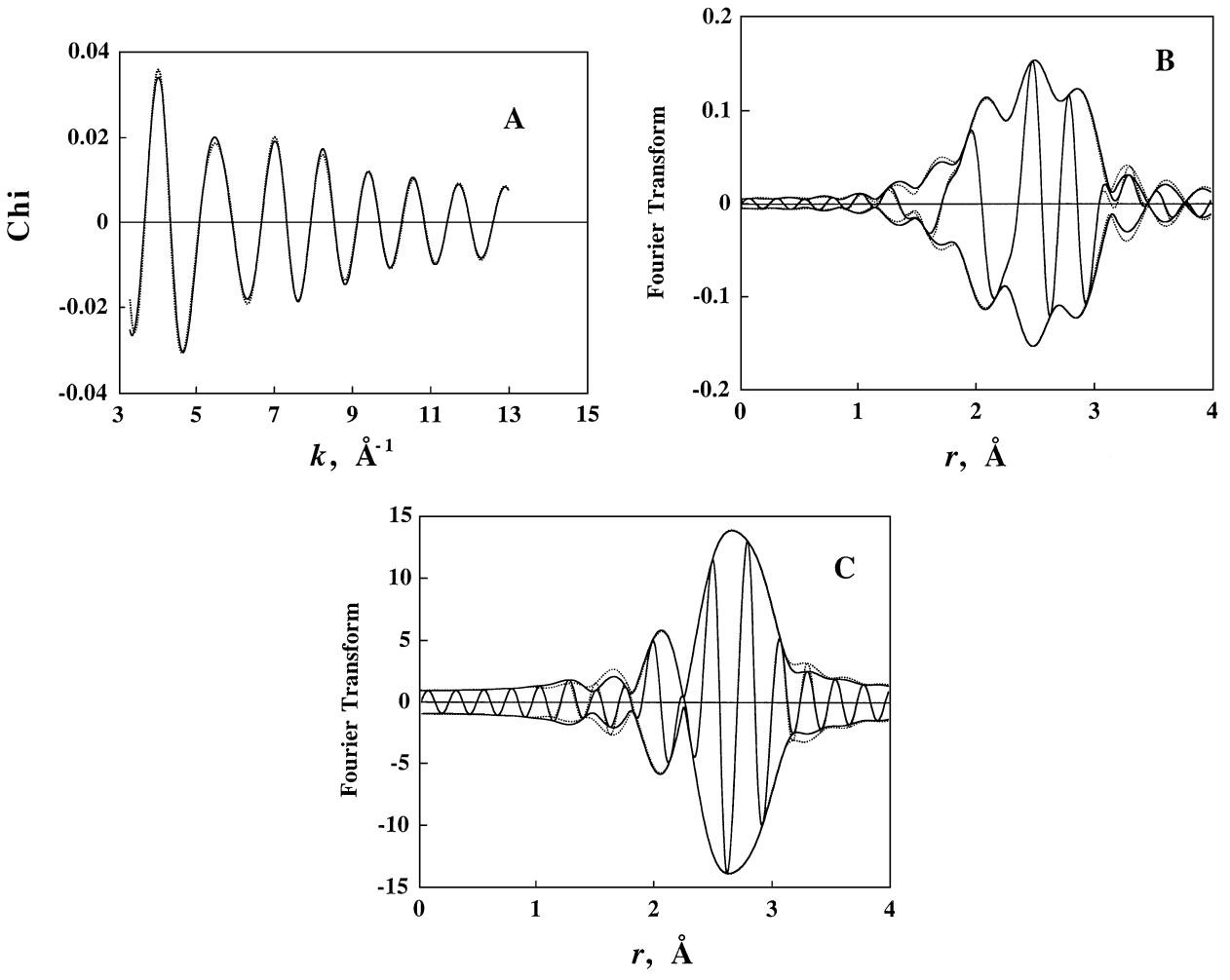

FIG. 10. Results of EXAFS analysis obtained with the best fitted structural parameters for the 1000 ppm sulfur-poisoned catalyst after 723 K hydrogenation reactivation: A, k^0-weighted experimental EXAFS (solid line) and sum of the calculated Pt–Pt plus Pt–S contributions (dashed line); B, imaginary part and magnitude of Fourier transform (k^1-weighted, $\Delta k = 3.5$–13.0 Å) of experimental EXAFS (solid line) and sum of the calculated Pt–Pt plus Pt–S contributions (dashed line); *C*, imaginary part and magnitude of Fourier transform (k^3-weighted, $\Delta k = 3.5$–13.0 Å) of experimental EXAFS (solid line) and sum of the calculated Pt–Pt and Pt–S contributions (dashed line).

in diesel has been reported and the results have been considered to be caused by the strong adsorption of aromatics on sulfur-poisoned Pt catalysts (4, 14).

By hydrogen reactivation, a drop in reaction order caused by sulfur-poisoning was restored. In contrast, the decrease of reaction rate constant caused by sulfur-poisoning was unable to be fully regained at the reactivation temperature up to 823 K (Table 3).

Infrared spectra characterizing sulfate on the Pt catalysts. Treatment of the sulfur-poisoned catalysts with oxygen leads to the transformation of sulfur species on the metal clusters into sulfate groups linked to the alumina support (18). The infrared spectra (Fig. 5) for the oxidation of the 500 ppm sulfur-poisoned catalyst are consistent with the presence of sulfate species. Moreover, after reactivating the catalysts with hydrogen at 823 K, the appearance of the small peak located at 1375 cm^{-1} in IR spectra characterizing the oxygen treated sample, suggests the deposition of residue sulfur on the catalyst sample. A chemical analysis of the sulfur content further indicates that about 15% of residue has not been removed after 823 K hydrogen treatment; the sulfur-poisoned catalyst contained 0.114 wt% sulfur, while the hydrogen-reactivated one contained 0.018 wt% sulfur. Paal *et al.* have reported the similar results and suggested that the difficulty in removing the deposition of sulfur on the catalysts because of its high resistance to customary chemical treatment is one of the reasons why the original activity was hard to be restored (15).

Characterization of CO adsorbed on the fresh, sulfur-poisoned, and hydrogen-reactivated catalysts. When CO

TABLE 2

Summary of Parameter Estimation Results for Sulfur-Poisoning Catalyst Deactivation

Sulfur concentration, ppm	k	n
0 (fresh catalyst)	10.7	0.98
100	7.9	0.97
250	6.2	0.93
500	3.8	0.57
1000	3.1	0.49

is adsorbed on the Pt clusters, electron transfer occurs from the *d*-orbitals of Pt to π^* (antibonding) orbital of CO (16). A sample with greater electron density on the platinum causes more backbonding from the metal to the CO π^*-orbital. This backbonding strengthens the Pt–C bond and weakens the C–O bond. As shown in Fig. 6a, FT-IR peak characterizing CO adsorbed on Pt clusters of the fresh catalyst sample is of one wave number at 2060 cm^{-1}. This peak was assigned as a terminal CO adsorption band (17), and it shifts about 80 cm^{-1} to a lower frequency, comparing the 2143 cm^{-1} characteristic of CO gas. For the sulfur-poisoned catalysts, an additional peak with an absorption frequency higher than that of CO adsorbed on the fresh catalyst was observed (Fig. 6). This band is also characteristic of a terminal CO adsorption band. The shift to higher frequency is consistent with the IR spectra characterizing CO adsorbed on sulfur-poisoned Pd catalysts, reported by Hoyos *et al*. (18) and is suggested to be a consequence of H_2S adsorbed on the Pt clusters, the residue sulfur deposited on the Pt clusters, and/or the formation of PtS. Those sulfur species, which abstract electron from Pt clusters (19), decrease the number of Pt electrons for π-bonding to CO, thereby weakening the electron-donation character and the Pt–C bond.

The absorption frequency increases with sulfur in the feed (2065 cm^{-1} for 100 ppm sulfur-poisoned catalyst sample and 2075 cm^{-1} for 1000 ppm sulfur-poisoned catalyst sample), whereas no significant variation in the ratio of the absorbance of the terminal CO adsorption band shifting to higher frequency to the absorbance of the total CO adsorption bands, $A_s/(A_L + A_s)$ has been observed (Table 4), where A_L is the absorbance of the terminal band at 2060 cm^{-1} and A_s is the absorbance of the band that shifts to higher frequency. The details of the chemistry for the change of CO adsorption spectra induced by sulfur-poisoning remain to be clarified. However, the correlation between ν_{CO} and the reaction order suggests a relation between electronic density of the Pt clusters and the reaction kinetics. The electron-donation character of tetralin may strengthen the affinity between electron-deficient Pt clusters and tetralin during sulfur-poisoning, leading to an increase in the tetralin-adsorption-equilibrium constant and a decrease in the observed reaction order.

TABLE 3

Summary of Parameter Estimation Results for Hydrogen Reactivation

Temperature (K)	k	n
Fresh catalyst	10.7	0.98
723	5.1	0.96
823	5.5	1.03

TABLE 4

Summary of CO Adsorption on the Fresh and the Sulfur-Poisoned Catalysts

Sulfur concentration	CO uptake (μmol/g of catalyst)/apparent dispersion (CO/Pt)	100 $A_s/(A_L + A_s)$ (%)
Fresh catalyst, 0 ppm	33.97/0.72	0
100 ppm	12.74/0.24	0.52
250 ppm	9.91/0.19	0.54
500 ppm	7.08/0.14	0.45
1000 ppm	6.61/0.13	0.50

In an attempt to reactivate the sulfur-poisoned catalysts, the 500-ppm sulfur-poisoned catalyst sample was treated with H_2, at temperature ranging from 723 to 823 K for 2 h. The electronic properties of the hydrogen-reactivated catalysts were examined by FT-IR characterizing CO adsorbed on the catalysts (Fig. 4). The relative intensity of the peak at 2070 cm^{-1} decreased with increasing temperature, while the peak at 2060 cm^{-1} increased. After 823 K hydrogen treatment, the spectra between the fresh and the hydrogen reactivated catalyst sample had only a slight difference (Figs. 4a and 4b), as shown in Tables 4 and 5; the value of $A_s/(A_L + A_s)$ decreases from about 0.5 to less than 0.1 after reactivation of the catalyst with the hydrogen at 823 K. The results suggested that the electron abstracted by sulfur species was restored after the hydrogen reactivation at 823 K. The regained electron may lessen tetralin

TABLE 5

Summary CO Adsorption on the Fresh Catalyst and the 500 ppm Sulfur-Poisoned Catalyst after Hydrogen Reactivation

Reactivation temperature (K)	CO uptake (μmol/g of catalyst)/apparent dispersion (CO/Pt)	100 $A_s/(A_L + A_s)$ (%)
Fresh	33.97/0.72	0
723	9.91/0.19	0.30
823	18.9/0.37	0.11

adsorption and release the catalyst from strong-adsorption poisoning.

XANES spectra. The intensity of the threshold resonance of the L_{III} edge (white line) is related to the transition probability of exciting inner-core 2p electrons into a vacant *d* valence level. Usually, the lower the electron density of the metal, the greater the number of vacancies in the valence level and, hence, the higher the probability of the transition or the higher the white line intensity (20). The near-edge absorption spectra (Fig. 8) show that the sulfur-poisoned catalysts exhibited a white line of slightly higher intensity than that of the hydrogen-reactivated one that the adsorbed H_2S have been removed. The decrease in while line intensity is small and is not conclusive evidence, but it is consistent with the increase of electron density of the platinum clusters after the hydrogen reactivation suggested by the FT-IR results.

EXAFS and chemisorption results. The FT-IR and kinetic results suggested a strong-adsorption-poisoning caused by the reduction of electron density induced by sulfur species. After the removal of H_2S and/or the reduction of PtS by hydrogen treatment, the lessening in electron density is recovered. Thus, we may optimistically expect that the activity loss by sulfur-poisoning will also be regained by hydrogen reactivation. However, the reverse was observed. Based on EXAFS, transmission electron microscopy (TEM), FT-IR and chemical analysis results (6, 11), we suggest that the activity that cannot be restored by hydrogen reactivation was caused by Pt agglomeration during sulfur-poisoning and the deposition of residue sulfur after hydrogen treatment.

Table 4 gives the amount of CO adsorbed on the fresh and sulfur-poisoned catalysts as a function of the severity of the sulfur poisoning. The results show that the CO adsorption is decreased with sulfur concentration and suggest that the decrease of the rate constant may be mainly caused by the loss of active sites (S^0); the possibility of the decrease of the surface reaction rate due to the change of electronic properties, however, may not be ruled out. The adsorption of H_2S, the formation of PtS, and the Pt agglomeration induced by sulfur-poisoning are considered to be the three major factors for the activity loss (6).

After hydrogen reactivation at 723 K, the amount of CO adsorbed on the catalysts was increased from 7.08 to 9.91 μmol CO/g of catalyst. Further, increasing the temperature to 823 K, the amount of CO adsorption was increased to 18.90 μmol CO/g of catalyst, but it was still lower than that by the initial Pt catalyst (Table 5). The results are consistent with the work of Hoyos *et al.* However, since no change in the Pd particle size have been found after the sulfur-treatment, Hoyos *et al.* attribute the decline of CO adsorption only to the sulfur atom deposition on the Pd surface (18).

In the previous paper, we reported that the Pt agglomeration may be caused by the decrease of Pt-support interactions and/or the formation of relatively mobile PtS (6). We also found that the sulfur resistance of Pt catalysts can greatly be enhanced by the addition of Pd (14). Together with the work of Hoyos *et al.* (18), we speculate that the Pd-support interactions may not be decreased by sulfur-poisoning and, thus, Pd helps anchor the Pt from migration and maintains it in a small ensemble during sulfur poisoning.

To investigate the effects of hydrogen reactivation on the structure of the catalysts, the Pt catalysts poisoned with 1000 ppm sulfur was reactivated at 723 K and characterized by EXAFS spectroscopy. In comparing the structural parameters and Pt–S contributions between the sulfur-poisoned and the hydrogen reactivated catalysts (Table 1 and Fig. 11), it indicates that after the hydrogen reactivation the coordination number for Pt–Pt and the Pt–S of bond distance at 2.33 Å is only slightly increased (within experimental error), whereas the peak of Pt–S contribution at 2.53 Å is vanished. Since the Pt–S with bond distance of 2.53 Å is assigned as the adsorption of H_2S on the Pt clusters, the disappearance of this peak (Fig. 11) suggests that the reversible adsorbed H_2S was removed after the hydrogen treatment.

In contrast to the sulfur-poisoning-induced Pt agglomeration reported in the previous paper (6), as shown in Fig. 12, the Fourier transform (k^3-weighted, Pt–Pt phase, and amplitude-corrected) peaks of the sulfur-poisoned and the hydrogen reactivated catalyst are almost identical in both position and intensity, indicating that there were no

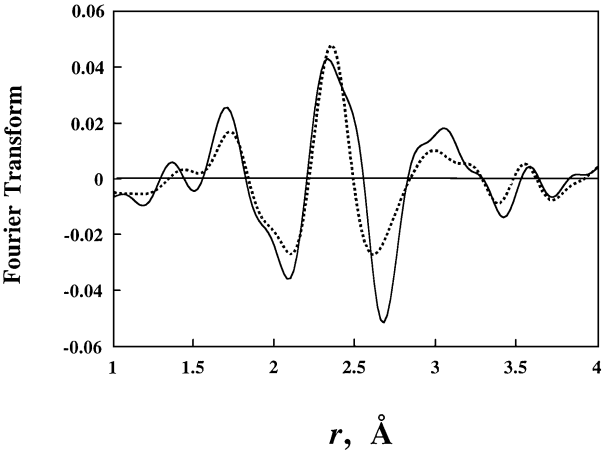

FIG. 11. Illustration of the low *Z* backscattering contributions for the 1000 ppm sulfur-poisoned catalyst and the catalyst after 723 K hydrogen reactivation: imaginary part of Fourier transform (k^1-weighted, Pt–Cl phase corrected, $\Delta k = 3.5$–13.0 Å) for original filtered EXAFS data of the 1000 ppm sulfur-poisoned catalyst minus calculated Pt–Pt EXAFS (solid line) and original filtered EXAFS data of the catalyst after 723 K hydrogen reactivation minus calculated Pt–Pt EXAFS (dashed line).

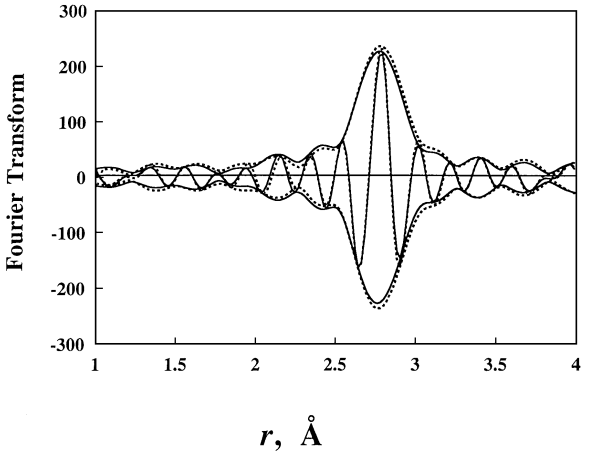

FIG. 12. Comparison of the normalized imaginary and magnitude of Fourier transforms (k^3-weighted, $\Delta k = 3.5$–16.0 Å, Pt–Pt phase and amplitude corrected) for the 1000 ppm sulfur-poisoned Pt/γ-Al_2O_3 catalysts (solid line) and the sulfur-poisoned catalysts after 723 K hydrogenation reactivation (dashed line).

significant morphology changes, of Pt clusters during the hydrogen reactivation process. These results indicated that the simple hydrogen reactivation method will not further induce the Pt agglomeration, but it also cannot redisperse the catalysts. A more complicated oxylchlorination method is necessary to redisperse the catalysts (21).

CONCLUSION

The structure of the catalysts were characterized by CO chemisorption and extended X-ray absorption fine structure (EXAFS) spectroscopy. Tested with sulfur-containing tetralin follows a pattern in which the reaction rate decreased with the severity of sulfur-poisoning. The decline of the reaction rate are caused by the formation of PtS, the adsorption of H_2S on the active sites, and the agglomeration of Pt particles. By hydrogen reactivation, the loss of catalyst activity cannot be regained completely because of the deposition of residue sulfur on the active sites and Pt agglomeration. The reaction results also indicated that the reaction order was decreased with increasing sulfur in feed. After hydrogen reactivation, the reaction order was increased and restored to that for the fresh catalysts. Inferred from FT-IR and XANES results, the decrease of the reaction order with sulfur concentration was considered to be caused by the increase of the tetralin-adsorption-equilibrium, resulting from an electron transfer from Pt to sulfur during sulfur-poisoning. By hydrogen reactivation, the change in electronic density of the Pt clusters and thus the reaction order was restored with the removal of H_2S and the reduction of PtS.

ACKNOWLEDGMENTS

The EXAFS data were analyzed using the XDAP Data Analysis Program, developed by M. Vaarkamp, J. C. Linders, and D. C. Koningsberger, and the reference files were provided by Dr. B. C. Gates. This research were supported by the National Science Council of the Republic of China (Contract NSC 85-2214-E-194-002) and by the Refining & Manufacturing Research Center of the Chinese Petroleum Corp. (RMRC). We are grateful to the staff of beam line X-11A at the National Synchrotron Light Source, USA, for their assistance. We also like to thank Dr. T.-B. Lin and Mr. W.-L. Chen of RMRC for their help with the chemical analysis of sulfur content and helpful discussion.

REFERENCES

1. Crow, P., and Williams, B., *Oil Gas J.* **Jan. 15** (1989).
2. UllMan, T. L., *in* "Soc. Automot. Eng., 1989," Paper 892072.
3. McCulloch, D. C., Edgar, M. D., Pistorious, J. T., *in* "NPRA Annual Meeting, March 1987," AM-87-58.
4. Stanislaus, A., and Cooper, B. H., *Catal. Rev.-Sci. Eng.* **36**(1), 75 (1994).
5. Cooper, B. H., Stanislaus, A., Hannerup, P. N., *Hydrocarbon Process.*, Jun 1993.
6. Chang, J.-R., Chang, S.-L., and Lin, T.-B., γ-alumina-supported Pt catalysts for aromatics reduction: A structural investigation of sulfur-poisoned catalyst deactivation, *J. Catal.* **169**, 338 (1997).
7. van Zon, F. B. M., *in* "A Structural Investigation of Supported Small Metal Particles and the Metal-Support Interface with EXAFS," p. 18. dissertation, Eindhoven University of Technology, The Netherlands, 1988.
8. van Zon, F. B. M., Maloney, S. D., Gates, B. C., and Koningsberger, D. C., *J. Am. Chem. Soc.* **115**, 10317 (1993).
9. Kampers, F. W. H., *in* "EXAFS in Catalysis: Instrumentation and Applications," dissertation, p. 26. Eindhoven University of Technology, The Netherlands, 1989.
10. Koningsberger, D. C., Prins, R., *in* "X-ray Absorption: Principles, Applications, Techniques of EXAFS, SEXAFS, and XANES," p. 395. Wiley, New York, 1988.
11. Chiou, J.-F., Huang, Y.-L., Lin, T.-B., Chang, J.-R., *Ind. Eng. Chem. Res.* **34**, 4277 (1995).
12. Boudart, M., *Chem. Eng. Prog.* **58**, 73 (1962).
13. Seinfeld, J. H., Lapidus, L., *in* "Mathematical Methods in Chemical Engineering. Process Modeling, Estimation, and Identification," Vol. 3, pp. 339–398. Prentice Hall, Englewood Cliffs, NJ, 1974.
14. Lin, T.-B., Jan, C.-A., Chang, J.-R., *Ind. Eng. Chem. Res.* **34**, 4284 (1995).
15. Paál, Z., Matusek, K., Muhler, M., *Applied catalysis A: General.* **149**, 113 (1997).
16. Cotton, F. A., Wilkinson, G., *in* "Advanced Inorganic Chemistry," pp. 58–68. John Wiley & Sons, 1988.
17. Little, L. H., Kiselev, A. V., Lygin, V. I., *in* "Infrared Spectra of Adsorbed Species," pp. 47–89. Academic Press: London and New York, 1966.
18. Hoyos, L. J., Primet, M., Praliaud, H., *J. Chem. Soc. Faraday Trans.* **88**, 3367 (1992).
19. Gallezot, P., Datka, J., Massardier, J., Primet, M., and Imelik, B., *in* "Proc. 6th Internat. Congress on Catalysis, London, 1976" (G. C. Bond, P. B. Wells, and F. C. Tompkins, Eds.), Vol. 2, p. 696. The Chemical Society, London, 1977.
20. Lytle, F. W., Wei, P. S. P., Greegor, R. B., Via, G. H., Sinfelt, J. H., *J. Chem. Phys.* **70**, 4849 (1979).
21. Fung, S. C., *CHEMTECH*, **Jan.**, 40 (1994).